
Wood-Frame Buildings: Numerical Study of an Envelope with Ventilated Walls

Gilles Fraisse, Ph.D.

Gilbert Achard, Ph.D.

V. Trillat-Berdal, Ph.D.

K. Johannes, Ph.D.

ABSTRACT

The objective of the study is to compare energy performances of different kinds of ventilated facades in the case of wood-frame buildings. The existing air gaps within this kind of building are a technical and financial advantage (easier installation). The principle of the ventilated facades (opaque or translucent) is to preheat fresh air by making it circulate in one or two serial air gaps. It leads to recovering in winter a part of heat losses through the envelope and of solar radiation. With regard to a nonventilated facade, global heat losses (walls and ventilation) are lower. A numerical modeling allows one to compare the energy performances of various ventilated walls: one or two serial air gaps, composition of the wall (layers), and glazed wall (increasing solar heat recovery).

INTRODUCTION

In France, construction with wood frame represents approximately 5% of residential houses. The wood construction is penalized by the lack of offers from builders. Nevertheless, wood construction presents numerous advantages on the environmental impact: CO₂ fixation, renewable raw material, reduction of construction site waste, material with lower embodied energy, etc. The advantage in using wood frame for ventilated walls is that air gaps already exist in such buildings. Many ventilated walls have been studied. Their interest is to preheat fresh air by the recovery of heat losses through the walls (Cadiergues et al. 1986) and of solar gains (IEA 2000). The first system means “dynamic insulation” and the second system is a “solar air system.” The two heat recovery systems reduce global heat losses (envelope and ventilation) and improve thermal comfort. A bypass is necessary in summer to limit the risks of overheating.

A well-developed solution in Canada for industrial buildings with large facades is the “solarwall” (unglazed transpired collector). The envelope consists of perforated panels made of either aluminium or galvanized steel. The metal panels are perforated with very small holes and are similar to a conven-

tional facade (Hollick 1996). Outside air is drawn through perforations and is sun-warmed. A ventilated facade, with one or two air gaps, works with opaque walls (Cadiergues et al. 1986; Thermophonie 1997; Stéphant 2002) and windows too (Baker and McEvoy 1999; Paziud 1997; Schmidt and Johansson 2002).

Two different dynamic insulation systems exist. The first one is called “parieto-dynamic” and concerns walls with air gaps. The other one, called “permeo-dynamic” system, consists in making the airflow cross through the insulation material when it is porous enough (Wallentén 1996). In this case, conductive heat losses through the wall are strongly reduced. However, this system presents risks toward air quality if molds, dusts, and bacteria develop within the insulation. Moreover, noxious microfibers may be emitted into the air.

Some systems retain the solar heat gains by making real glazed solar collectors within the building envelope (Pottlers et al. 1999; Ubertini and Desideri 2003). These solutions use a black absorber whereas the insulating layer of the existing wall limits the backward losses (inward of the building). In the case of windows, the absorber (moveable blind) can be put between two glazings (IEA 2000). The Trombe wall (of

Gilles Fraisse is an associate professor, Gilbert Achard is a professor, and Valentin Trillat-Berdal and Kevyn Johannes are graduate students in the University of Savoy, ESIGEC, Design Optimisation and Environmental Engineering Laboratory.

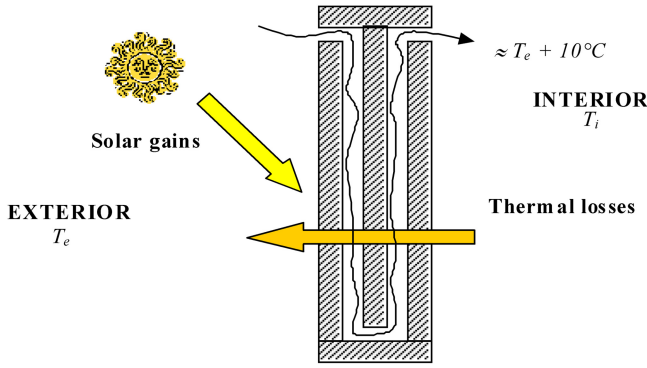


Figure 1 Functioning principle of the VW.

professor F. Trombe and architect J. Michel) with an external glazing and a massive concrete wall allows delay of solar heat transmission inwards (Trombe 1971). In this case, air flow is due to natural convection. Finally, the principle of double-skin facade consists of adding a second transparent envelope on the existing one (IEA 2000). This creates a buffer zone that reduces thermal losses.

These systems could be designated as helio-parietodynamic walls since solar radiation and thermal losses increase ventilation air temperature (Stéphane 2002). A solar collector designates a system that is designed to increase solar gains (for example with external glazing).

This study is part of a project with the aim of improving the energy performance and the thermal comfort of wood-frame buildings. The presented results only concern the reduction of the heating loads. The principle is to preheat ventilation air using air gaps within ventilated walls (VW). The flow rate (air speed) within VW is determined by the ventilation rate. The airflow goes inside because of the negative pressure created by the fan of the extract ventilation system. Therefore, there is no additional fan or control system.

BEHAVIOR OF A VENTILATED WALL

A ventilated wall allows air to circulate inside a wall so that the wall acts as a heat exchanger between interior and exterior (Figure 1). The incoming air is warmed in winter because of the thermal losses through the wall and the solar gains. The thermal efficiency of a VW increases with the number of serial air gaps (Trillat-Berdal 2003).

The advantages of a ventilated envelope include the possibility of evacuating the heat in summer, the improvement of thermal comfort in winter by avoiding cold air drafts, the reduction of heat losses, and the improvement of sound proofing. On the other hand, the implementation of a VW entails additional costs. Furthermore, the installation for flow distribution in the VW and air leakage must be carefully achieved because it determines the final energy performance. In the case of ventilated windows, a regular cleaning is necessary, whereas VW can accumulate some dust within the air gaps.

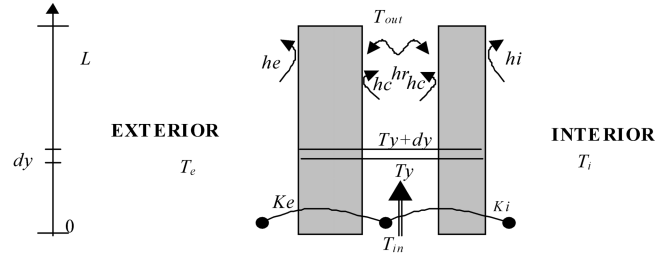


Figure 2 VW with one air gap.

Finally, it is essential to bypass the VW in summer to avoid overheating.

Steady-State Modelling (One Air Gap)

For a VW with one air gap between two parallel walls, as shown in Figure 2, the outlet air temperature T_{out} can be calculated by the integration of the energy balance of a dy thickness layer from the bottom ($y = 0$) to the top ($y = L$) (Duffie and Beckman 1991; Schmidt and Johannesson 2002). The inlet temperature (T_{in}) and the heat transfer coefficients (hc and hr) are assumed to be constants.

$$T_{out} = \frac{K_e \cdot T_e + K_i \cdot T_i}{K_e + K_i} \gamma + T_{in} \cdot \exp(-\alpha \cdot L) \quad (1)$$

$$\alpha = \frac{hc \cdot (hc + 2hr)}{hr \cdot Qm \cdot Ca} \cdot \frac{K_e + K_i}{K_e + K_i + \frac{hc \cdot (hc + 2hr)}{hr}} \quad (2)$$

$$\frac{1}{K_e} = \frac{1}{h_e} + R_{wall1} + \frac{1}{hc + 2 \cdot hr} \quad (3)$$

and

$$\frac{1}{K_i} = \frac{1}{h_i} + R_{wall2} + \frac{1}{hc + 2 \cdot hr} \quad (4)$$

$$\gamma = 1 - \exp(-\alpha \cdot L) \quad (5)$$

where

hc and hr = convective and radiative heat transfer coefficient, W/m^2K

T_i and T_e = internal and external temperature, $^{\circ}C$

h_i and h_e = global internal and external heat transfer coefficient, W/m^2K

Qm = air mass flow rate, kg/s

Ca = specific heat of the air, $J/kg K$

The heat recovery rate by air between the input and output is:

$$\Phi = Qm \cdot Ca \cdot (T_{out} - T_{in}) = Qm \cdot Ca \cdot \gamma \cdot \frac{K}{K_e} \cdot (T_i - T_e) \quad (6)$$

where

$$K = \frac{Ki \cdot Ke}{Ki + Ke} \text{ [W/m}^2\text{K]}$$

Considering that the mass flow rate Qm equals the ventilation airflow rate, the ventilation heat losses Φ_V and the thermal losses through the VW Φ_{VW} are :

$$\Phi_V = Qm \cdot Ca \cdot (T_i - T_{out}) = \Phi'_V - Qm \cdot Ca \cdot \frac{K}{Ke} \cdot \gamma \cdot (T_i - T_e) \quad (7)$$

$$\Phi_{VW} = \Phi'_{VW} + Qm \cdot Ca \cdot \left(\frac{K}{Ke}\right)^2 \cdot \gamma \cdot (T_i - T_e) \quad (8)$$

In a classic configuration where the air enters the house directly, the corresponding ventilation and thermal heat losses are:

$$\Phi'_V = Qm \cdot Ca \cdot (T_i - T_e) \quad (9)$$

and

$$\Phi'_{VW} = K \cdot A \cdot (T_i - T_e) \quad (10)$$

where

A = wall surface, m²

The difference between the two configurations is:

$$\begin{aligned} \Delta\Phi &= \Phi'_{VW} + \Phi'_V - \Phi_{VW} - \Phi_V = \\ Qm \cdot Ca \cdot \frac{K}{Ke} \cdot \left(1 - \frac{K}{Ke}\right) \cdot \gamma \cdot (T_i - T_e) &> 0 \end{aligned} \quad (11)$$

The positive difference indicates that the airflow through the wall systematically reduces the global thermal losses (envelope and ventilation). The maximum difference is obtained in the case of a symmetrical wall, i.e.,

$$\frac{K}{Ke} = 0.5 \quad (12)$$

Concerning the global balance, the ventilated wall is equivalent to a classic configuration for which the wall would have a conductance K_{dyn} lower than the conductance K of the wall without air circulation:

$$K_{dyn} = K \cdot \left(1 - \frac{Qm \cdot Ca}{A} \cdot \frac{\gamma}{Ki + Ke}\right) \quad (13)$$

It is important to note that the reduction in the global heat losses results from the ventilation heat recovery being greater than the heat conduction losses through the VW:

$$\Phi'_{VW} < \Phi_{VW} \text{ and } \Phi'_V > \Phi_V$$

It's possible to use an heat exchanger (HX) and a VW to preheat fresh air. We are going to see that the global performance in the case of HX+VW is not necessarily better than the

HX case (without any VW). In this case, the heat rate recovered is:

$$\Phi_V^{HX} = \eta \cdot Qm \cdot Ca \cdot (T_i - T_e) \quad (14)$$

where

η = temperature efficiency of air to air heat exchanger (supposed constant).

In case the heat exchanger is after the VW, the recovered heat rate is:

$$\Phi_V^{dyn+HX} = \eta \cdot Qm \cdot Ca \cdot (T_i - T_{out}) + Qm \cdot Ca \cdot (T_{out} - T_e) \quad (15)$$

Considering the heat losses through the VW, noted, the difference is:

$$\Phi_V^{dyn+HX} - \Delta\Phi_{VW}^{dyn} - \Phi_V^{HX} = (\Phi'_V - \Phi_V) \cdot \left(1 - \eta - \frac{K}{Ke}\right) \quad (16)$$

If the heat exchange has an efficiency $\eta = 1$, it is evident that it is useless to use a VW because the supply air temperature is equal to the internal temperature. For a value $\eta = 0.6$ (Roulet et al. 2001) and an optimal configuration for the VW ($K/Ke = 0.5$), we obtain:

$$1 - \eta - \frac{K}{Ke} = -0.1 < 0 \quad (17)$$

This means that the energy saving is larger when we use the heat exchanger alone (without any VW)! This is due to the increase of heat conduction through the VW. This increase is less important for low values of Ke . The optimal configuration is interesting to limit the risk of frost in the heat exchanger (Hollmuller 2002).

The results obtained until now do not integrate the solar gains. Let us consider the equivalent external temperature T_{eq} with solar gains considered:

$$T_{eq} = T_e + \frac{\alpha_e \cdot E}{he} \quad (18)$$

where

α_e = absorptance of the outside face

E = solar radiation, W/m²

With a similar derivation presented in Equations 1 to 16, the difference between the two configurations $\Delta\Phi_{sol}$ (with solar gains) is

$$\Delta\Phi_{sol} = Qm \cdot Ca \cdot \gamma \cdot \left(1 - \frac{K}{Ke}\right) \cdot \left(\frac{K}{Ke} \cdot (T_i - T_{eq}) + \frac{\alpha_e \cdot E}{he}\right) \quad (19)$$

Figure 3 shows, as a function of K/Ke , the heat loss reduction $\Delta\Phi_{sol}$ with regard to the maximal heat reduction ($K/Ke = 0.5$) obtained when solar irradiation E is equal to zero. When E increases, the optimal value (maximum $\Delta\Phi_{sol}$) of Ke

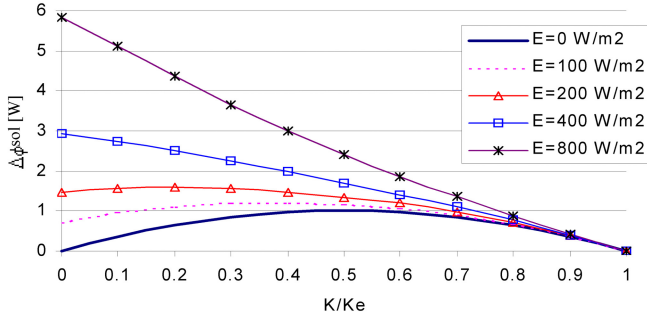


Figure 3 Energy savings as a function of the wall composition.

decreases (internal side insulation). The values of $\Delta\Phi_{sol}$ show that solar gains have an important influence.

Non-Steady-State Modeling (One or Two Air Gaps)

To determine the actual heat loads under real weather conditions, it is important to consider the inertia of the wall. The conductive heat transfers of a VW with one air gap are modeled by the network technique, as shown in Figure 4. A 3R2C model (3 resistances and 2 capacitances) is used. A capacitance is added to each wall face to take into account the conductive heat exchanges close to each face for small time steps more precisely (Fraisie et al. 2002).

The previous approach is used considering only the air gap. The surface temperatures $T4$ and $T6$ (nodes 4 and 6 of the RC model) are supposed to be average VW temperatures. Besides, we distinguish the outside air temperature T_e and the sky temperature T_c in order to better take into account the convective and long wave radiation (cooling due to the sky temperature). Also, the room is characterized by an air temperature T_a and a mean radiant temperature T_{rm} .

In these conditions, the outlet air temperature is:

$$T_{out} = \frac{T4 + 6T}{2} \gamma + T_{in} \cdot \exp(-\alpha \cdot L) \quad (20)$$

The heat rate $\phi5$ corresponds to the air enthalpy difference between bottom and top of the VW. The heat rates $\phi1$ and $\phi9$ are solar gains.

$$\phi5 = Qm \cdot Ca \cdot (T_{in} - T_{out}) < 0 \quad (21)$$

The conductances inside the air gap are:

$$K4 = K5 = hc + 2 hr \quad (hc \text{ and } hr \text{ are assumed constant}) \quad (22)$$

The radiative heat transfer coefficient hr is:

$$hr = \frac{\sigma_o \cdot (T_4^2 + T_6^2) \cdot (T_4 + T_6)}{\frac{1}{\epsilon_4} + \frac{1}{\epsilon_6} - 1} \quad (23)$$

where

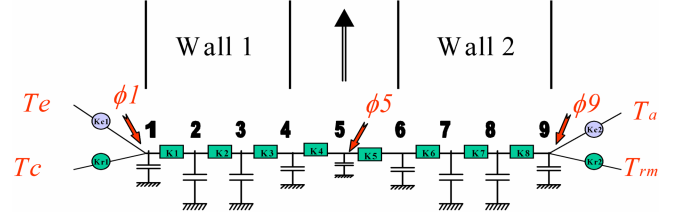


Figure 4 VW network model for one air gap (TRNSYS model: TYPE 94.FOR).

$$\sigma_o = 5.67 \cdot 10^{-8} \text{ W/m}^2\text{K}^4 \quad (\text{Stephan Boltzman constant})$$

The expression of the convective heat transfer coefficient in the air gap depends on the regime: laminar, transition, and turbulent. The heat transfer coefficient is calculated according to the Nusselt number Nu , the air thermal conductivity λ_a and the hydraulic diameter D_H of the air gap (ASHRAE 1997):

$$hc = \frac{Nu \times \lambda_a}{D_H} \quad (24)$$

and

$$D_H = \frac{4 \cdot S}{P} \approx 2 \cdot e \quad (25)$$

where

- e = air gap thickness, m
- S = air gap section, m^2
- P = perimeter of the air gap, m
- Nu = Nusselt number,

The literature gives numerous examples of Nusselt number calculation for forced convection in an air gap between two flat plates or in a rectangular section. These papers notably concern sol-air air collectors (Ong 1995; Njomo 1998; Pottler et al. 1999; Ubertini and Desideri 2003; Ammari 2003), airflow in ducts (Hollmuller 2002), solar air heating floors (Becker 1995), ventilated walls (Breton 1986; Schmidt and Johannesson 2002), and hybrid photovoltaic/thermal collectors (Guiavarch 2003; Mei et al. 2003).

The nine differential equations, defined from the energy balance of every node of the model (Figure 4), are solved at each time step. The temporal discretization is achieved with a fully implicit scheme, which presents the advantage to be unconditionally stable.

The double air gap is also considered (TRNSYS model: TYPE70.FOR). The approach remains identical to the case with one air gap. The input air temperature may be the external temperature or the outlet temperature of another air gap (case of a double air gap).

Table 1. The Studied Cases and Their VW Characteristics

REF	Reference case without any VW: Wood (2 cm, $\alpha_{SWR}=0.6$), air gap (3cm), wood (1cm), insulation (12 cm), plaster (1.3 cm) External wall 128 m ² (nonventilated) Air ventilation (100 m ³ /h for 22 hours a day, 180 m ³ /h for 2 hours)
REF/HX	Same as REF + heat exchanger fresh air / exhaust air ($\eta=0.6$)
NSEW	Ventilated wall for all facades: (120 m²) Same as REF + ventilated air gap $hc=2.4$ W/m ² K, $hr=5$ W/m ² K, and flow rate 100/180 m ³ /h VW : south (35m ²) + north (35m ²) + east (17 m ²) + west (32m ²) Nonventilated external wall: 8 m ²
NSEW/SYM	symmetrical wall : optimized heat loss recovery through the VW Same as NSEW, $K/Ke=0.5$ (insulation 6 cm + ventilated air gap + insulation 6 cm)
SOUTH	South-facing ventilated wall : (35m²) Same as NSEW /SYM, south-facing VW (35 m ² - south)
SOUTH /HX	Same as SOUTH, heat exchanger ($\eta=0.6$)
SOUTH /2	Same as SOUTH + double air gap obtained with 11 cm brick and a 3 cm ventilated air gap
COL/OVER	South-facing glazed collector (nonselective absorber): (2 m²) Air flow over the absorber ($\alpha_{SWR}=0.9$, $\varepsilon_{LWR}=0.9$, $hr=5$ W/m ² K)
COL /UNDER	Same as REF + ventilated air gap ($hc=5.3$ W/m ² K) and external wood is replaced with glazing Same as COL/OVER + ventilated air gap ($hc=5.3$ W/m ² K) under the absorber Nonventilated air gap between glazing and absorber
COL / UNDER /HX	Same as COL/UNDER, heat exchanger ($\eta=0.6$)

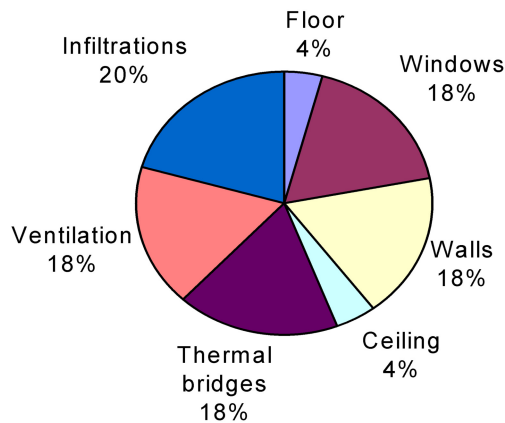


Figure 5 Distribution of heat losses.

NUMERICAL SIMULATIONS

The simulated building is a single-family dwelling of 120 m² and is located in Mâcon (2580 HDD). The inertia is very low as we consider a wood frame (the time constant is 25 h). The thickness of insulation is 12 cm for outside walls, 13 cm for the floor (over a ventilated space), and 17 cm for the ceiling. The window thermal conductance is 2.8 W/m²K. The insulation level of the house corresponds to the level of the French thermal regulation (CSTB 2001). The heating loads are 90 kWh/m²_{floor} year. The internal and external gains cover 34% of the total heating loads.

The new French thermal regulation leads to reduced heat losses through the walls. Consequently, the interest of dynamic insulation decreases. In these conditions, heat recovery of solar gains is of more interest. As a comparison, the south facade (vertical) of the studied house receives 500 kWh/m² during the heating season, while the heat losses through the walls are only 17 kWh/m² ($K = 0.27$ W/m²K and the number of degree-days is 2580).

The study is carried out using the TRNSYS software (Klein et al. 1996). This software is widely used by the international scientific community in the energy and thermal domain. This software is based on connecting elementary modules called TYPE, which are either components of the studied system or particular functions (weather data reader, etc.).

Case Studies

All the case studies are summarized in Table 1, along with the characteristics of the VW (layers from outside to inside).

The airflow rate through the ventilated wall is determined by the ventilation air change rate. The area of the glazed collector (COL) was defined from the current value of 50 m³/h·m² collector (IEA 2000). Other cases were studied (selective absorber, etc.) and the results will be given as comparison.

Energy Balances

Figure 5 shows the distribution of the thermal losses (reference case REF) through all the envelope components (13265 kWh during the heating season). Henceforth, the external walls do not offer an important potential of recovery because of the thermal regulation RT2000 (reduction in the

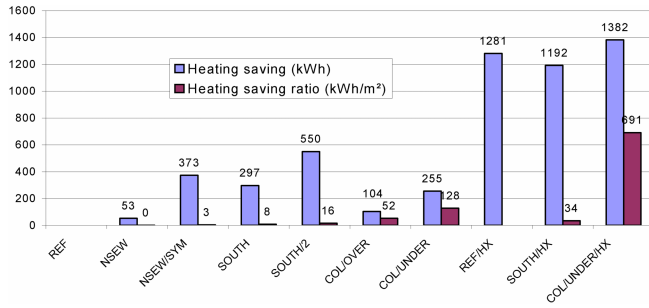


Figure 6 Heating savings.

wall conductance coefficient K). However, air infiltration (weak point of house with wood frame) and thermal bridges (limited because of the low thermal conductivity of wood) offer an important potential of energy savings.

In the reference case, heating loads are 10851 kWh. The heating energy savings, compared to the reference case REF, are presented in Figure 6, as well as the heating saving ratio (energy savings over area). This ratio defines the energy performance of the system and gives information about the cost and the difficulty of the installation.

The comparison of the savings for NSEW and NSEW/SYM ($K/Ke \approx 0.5$) cases confirms the results obtained in steady-state regime. The saving with NSEW/SYM is seven times higher than for the initial wall (NSEW). Because of the large area, the heating saving per square meter is very low in both cases.

The SOUTH case (35 m²) uses only 35% of the NSEW/SYM VW area (120 m²). Nevertheless, the SOUTH case (297 kWh) achieves 80% of the NSEW/SYM energy savings (373 kWh). The ratio is naturally increased because of the reduction of the area (8 kWh/m²). With regard to the SOUTH case (one air gap), the double air gap wall almost doubles savings (the thermal resistance of brick contributes to it partially).

For the glazed collector cases (COL, 2 m² south facing), the airflow under the absorber (UNDER), instead of over the absorber (OVER), is obviously more effective (losses toward surrounding reduced). The heating savings are 255 kWh and 345 kWh, respectively, for the COL/UNDER case (no selective absorber) and a case with selective absorber $\epsilon_{LWR}=0.2$ (not shown in Figure 6). It is also possible to increase savings by modifying the area of the COL cases (from 255 kWh with 2 m² for COL/UNDER to 766 kWh for 10 m²).

It is very interesting to compare the heating load with and without a heat exchanger. The case with both heat exchanger and VW (SOUTH/HX) gives heating savings (1192 kWh) lower than the case using heat exchanger alone (1281 kWh). The reason is shown in Figure 7: the extra heat losses due to the VW are large (372 kWh). It is interesting from an energy point of view to combine a collector with a heat exchanger (COL/UNDER/HX).

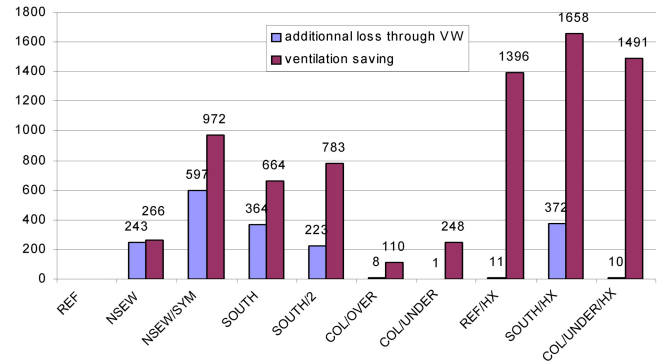


Figure 7 Reduction of ventilation heat losses and extra heat losses through the VW (kWh).

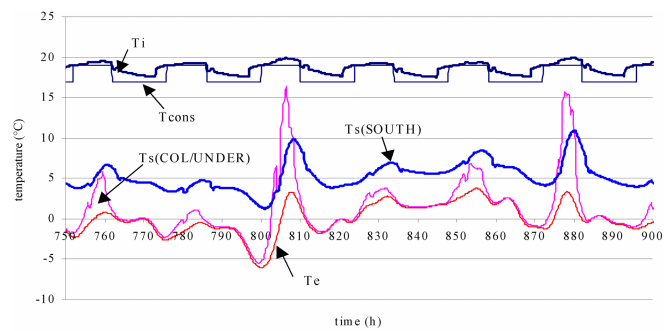


Figure 8 Temperature profiles.

For the same area (120 m²), the NSEW/SYM solution gives higher heat losses through the VW because the air gap position is closer to the interior. The VW with a double air gap (SOUTH/2) allows one to reduce both heat losses through VW and ventilation heat losses (Costa et al. 2000).

Temperature Profiles

Figure 8 shows the temporal profile of external temperature (T_e), internal temperature (T_i), and supply air temperature T_s for the cases SOUTH (35 m² of south VW) and COL/UNDER (2 m² of south glazed collector). The case SOUTH allows one to obtain an almost constant difference $T_s - T_e$ ($\approx 5^\circ\text{C}$). For the COL/UNDER case, the difference $T_s - T_e$ depends directly on the solar radiation. It is thus impossible to eliminate the risk of frost in the case of a coupling with heat exchanger.

CONCLUSIONS

A comparison of different VW was achieved in the case of a single-family dwelling with wood-frame construction. The potential of a dynamic insulation favoring the recovery of heat losses through VW exists if the wall was correctly defined ($K/Ke = 0.5$). It is possible to use only the south-facing orientation without significant reduction of energy saving. In that case, the case of a double air gap is better because of heat loss reduction through the VW.

The comparison of heat losses and solar gains for a south-facing wall puts in evidence a more important potential of recovery with regard to solar radiation. Moreover, the thermal regulation (RT2000) leads to small conductive heat losses through the walls. In these conditions, it is worth using a glazed VW with airflow under the absorber. Furthermore, the case limits the system area while keeping an important potential of savings. This point is very important because of the difficulty of controlling airflow for large VW. The drawback of such a system is that the energy saving is available only during sunny periods.

Now, we are working on a facade integrated collector located before a massive ventilated internal wall. It is the principle of murocaust (Bansal and Shail 1999) applied to fresh air preheating as ventilation air inlets are on the massive wall. The advantage is to preheat fresh air two times (collector/massive wall) or to cool fresh air because of the wall inertia if air is too warm. In summer, the thermal comfort should be improved because of the wall inertia.

ACKNOWLEDGMENTS

This study is financed by ADEME-PUCA in the framework of the program “Energy, Environmental and Sanitary Quality: to Prepare the Building to the 2010 Horizon.”

NOMENCLATURE

A	= wall area, m ²
Ca	= specific heat of the air, J/kg K
E	= solar radiation, W/m ²
e	= air gap thickness, m
hc	= convective heat transfer coefficient in air gap, W/m ² K
he	= global external heat transfer coefficient, W/m ² K
hi	= global internal heat transfer coefficient, W/m ² K
hr	= radiative heat transfer coefficient in air gap, W/m ² K
K	= conductance of the wall, W/m ² K
Ke	= conductance between air gap and exterior, W/m ² K
Ki	= conductance between air gap and interior, W/m ² K
L	= height of the ventilated wall, m
Nu	= Nusselt number
P	= perimeter of the air gap, m
Qm	= mass flow rate, kg/s
S	= section of the air gap, m ²
Ta	= internal air temperature, °C
Tc	= sky temperature, °C
Te	= external temperature, °C
Teq	= external equivalent temperature, °C
Ti	= internal temperature, °C
Tin	= input temperature, °C
$Tout$	= output temperature, °C
Trm	= mean radiant temperature, °C

α_e	= external absorptance
ϵ	= emissivity
η	= air to air heat exchanger efficiency
Φ_{VW}	= heat losses through the VW, W
Φ_V	= ventilation heat losses, W
Φ^{dyn}	= global losses in the case of VW system, W
Φ^{dyn+HX}	= global losses in the case of VW + HX system, W
σ_o	= Stephan Boltzman constant, W/m ² K ⁴

REFERENCES

- Ammari, H.D. 2003. A mathematical model of thermal performance of a solar air heater with slats. *Renewable Energy* 28(10): 1597-1615.
- ASHRAE. 1997. *1997 ASHRAE Handbook—Fundamentals*, SI Edition. Atlanta: American Society of Heating, Refrigerating and Air-Conditioning Engineers, Inc.
- Baker, P.H., and M.E. McEvoy. 1999. An investigation into the use of a supply air window as a heat reclaim device. *Proceedings of CIBSE A: Building Services and Engineering Technology* 20(3): 105-112.
- Bansal, N.K., and Shail. 1998. Characteristic parameters of a hypocaust construction. *Building and Environment* 34(3): 305-318.
- Becker, R. 1995. Computational model for analysis of dynamic thermal performance of a hybrid slab-collector system with passive discharge. *Solar Energy* 55(6): 419-433.
- Breton, J. 1986. Modélisation thermique et simulation numérique en régime variable de parois à lame d'air insolée et/ou ventilée. Thèse de INSA de Lyon, 363 p.
- Cadiergues, R., R. Espic, M.C. Lemaire, and E. Michel. 1986. Isolation dynamique, étude de synthèse, rapport final, contrat n°4.330.2315, 217 p.
- Costa, M., et al. 2000. Optimal design of multi-functional ventilated facades. Final report. Contract JOR3-CT98-0190, Non nuclear Energy Programme Joule III.
- CSTB. 2001. Réglementation thermique, guide RT2000, Enjeux, changements, exigence, textes de référence, <http://www.cstb.fr>.
- Duffie, J.A., and W.A. Beckman. 1991. *Solar Engineering of Thermal Processes*, 2d ed. New York: Wiley Intersciences.
- Fraisse, G., C. Viardot, O. Lafabrie, and G. Achard. 2002. Development of a simplified and accurate building model based on electrical analogy. *Energy and Building* 1430, p. 1-14.
- Guiavarch, A. 2003. Etude de l'amélioration de la qualité environnementale du bâtiment par intégration de composants solaires. Thèse de l'université de Cergy-Pontoise et de l'Ecole des Mines de Paris, 311 p.
- Hollick, J.C. 1996. World's largest and tallest solar recladding. *Renewable Energy* 9, Issues 1-4, pp. 703-707.

- Hollmuller, P. 2002. Utilisation des échangeurs air/sol pour le chauffage et le rafraîchissement des bâtiments. Thèse de l'Université de Genève, 126 p.
- IEA. 2000. *Solar air systems: A design handbook*. Ed. R Hastings. IEA Solar Heating and Cooling Programme. Published by James & James.
- Klein, S.A., et al. 1996. TRNSYS, a transient system simulation program, version 14.2. Solar Energy Laboratory, University of Wisconsin-Madison, reference manual, WI 53706.
- Mei, L., D. Infield, U. Eicker, and V. Fux. 2003. Thermal modelling of a building with an integrated ventilated PV façade. *Energy and Buildings* 35(6): 605-617.
- Njomo, D. 1998. Thermal behaviour of a combined plastic-glass flat plate solar air collector. *Revue Générale de Thermique* 37(11): 973-984.
- Ong S.K. 1995. Thermal performance of solar air heaters--experimental correlation. *Solar Energy* 55(3): 209-220.
- Paziaud, J. 1997. Des fenêtres pariéto-dynamiques contre les déperditions thermiques. *Les Cahiers Techniques du Bâtiment*, n°181, p 38-40.
- Pottler, K., C. M. Sippel, A. Beck, and J. Fricke. 1999. Optimized finned absorber geometries for solar air heating collectors. *Solar Energy* 67, Issues 1-3, pp. 35-52.
- Roulet, C.A., F.D. Heidt, F. Foradini, and M-C. Pibiri. 2001. Real heat recovery with air handling units. *Energy and Buildings* 33(5): 495-502.
- Schmidt, D., and G. Jóhannesson. 2002. Approach for modelling of hybrid heating and cooling components with optimised RC networks. *The Nordic Journal of Building Physics*, Vol. 3, 34 p.
- Shah, R.K., and A.L. London. 1978. *Laminar Flow Forced convection in ducts*. New York: Academic Press.
- Stéphane, J.P. 2002. Les façades à effet helio-pariéto-dynamique, *Techni.Cités*, n° 23, 2 p.
- Thermophonie. 1997. L'art du bâti, les isolations dynamiques, fiches et produits systèmes dynamiques. 36 p.
- Trillat-Berdal, V. 2003. Enveloppe pariéto-dynamique des maisons à structure bois. Diplôme d'Etudes Approfondies, Ecole Supérieure d'ingénieurs de Chambéry, 103 p.
- Trombe, F. 1971. Brevet ANVAR Trombe-Michel BF 7123778, France.
- Ubertini, S., and U. Desideri. 2003. Design of a solar collector for year-round climatization. *Renewable Energy* 28(4): 623-645.
- Wallentén, P. 1996. Dynamic insulation, analysis and field measurements. Report TABK—96/3034, Lund University, Sweden. 36 p.